
A Recipe to Couple Two Finite Volume Schemes for Elliptic Problems

Jérôme Droniou

*Département de Mathématiques, UMR CNRS 5149, CC 051,
Université Montpellier II, Place Eugène Bataillon,
34095 Montpellier cedex 5, France.*

email: droniou@math.univ-montp2.fr

ABSTRACT. We propose and study a method to discretize linear second order elliptic equations on a domain Ω using any two finite volume schemes, each scheme being applied on a different region of Ω . We point out general properties of finite volume schemes which allow us to prove the well-posedness and convergence of the method, and we provide numerical results, involving two particular schemes, to show its efficiency.

KEYWORDS: elliptic equations, finite volume schemes, coupling, irregular grids, anisotropy, heterogeneity, cost efficiency, mixed finite volume method.

1. Introduction

Finite volume schemes are widely used to discretize diffusion problems; they have several features, such as the conservation of various physical quantities, which makes them popular in some engineering fields. The basic schemes (see [EYM 00]) are easy to implement and cost-effective (in terms of memory and CPU time) but can only be applied on grids which satisfy some “admissibility” conditions (linking the geometry of the grid with the operator in the equation); other schemes (such as in [AAV 98, DOM 05, DRO 06-2, LEP 05]) can be applied on very general grids, but are much less cost-effective.

In several situations, the considered grids are “non-admissible” only in part of the domain; in this case, it does not seem wise to use an expensive scheme on the whole domain, but only in the non-admissible part of the grid, and to use a simpler scheme where possible. The aim of this paper is to present a general framework to achieve exactly this: to discretize an equation by applying two different finite volume schemes in two different regions. The ideas we use are quite general, but for the sake

of legibility we present them using the following model of a second order elliptic problem with Dirichlet boundary conditions:

$$-\operatorname{div}(A\nabla u) = f \quad \text{in } \Omega, \quad [1]$$

$$u = g \quad \text{on } \partial\Omega, \quad [2]$$

where Ω is a bounded polygonal open subset of \mathbb{R}^d and $f \in L^2(\Omega)$. Since we will only consider generic finite volume methods (see below), the precise assumptions regarding the rest of the data is not important here (it only matters that, when taking specific schemes, the data are compatible with those schemes).

Up until the numerical results presented in section 5, we intend to handle each finite volume scheme as a black box: in order to build a general framework, we will not consider the precise way each scheme is written, but rather the main features finite volume schemes usually possess (basic unknowns, convergence properties, etc.). Section 2 is devoted to a general presentation of finite volume methods for elliptic problems and their core unknowns and relations. In section 3, we present the coupling of two schemes, i.e. a way to discretize [1]–[2] by applying two finite volume schemes on two different subdomains, using no more information on these schemes than the basic information from section 2. We are then interested in the proof that such a coupling works; the studies of convergence of various finite volume methods usually rely on the same techniques (*a priori* estimates, compactness properties of the approximate solution, proof that its limit is a solution to the PDE): in section 4, we show that if each scheme, independently of the other and of any coupling consideration, enjoys such properties, then the scheme obtained by coupling both has a unique solution which converges to the solution of the continuous equation. Hence the “black box” idea mentioned above: we only use the convergence properties of each scheme, not their precise expression, to ensure the convergence of the coupling... at least in theory, but the numerical experiments provided in section 5 also show its practical efficiency.

In order to retain enough space for the presentation of several numerical results, the proofs of the theorems stated below are only sketched here; full proofs will be included in a forthcoming paper.

2. Core elements of finite volume schemes for elliptic problems

Finite volume schemes for a second order boundary value problem such as [1]–[2] are usually built along the following guidelines.

Discretization of Ω : a discretization \mathcal{D} of the domain consists as a minimum of a partition \mathcal{M} of Ω in polygonal open sets K (the control volumes) and a set \mathcal{E} of edges σ . Denoting by \mathcal{E}_K the set of edges ⁽¹⁾ contained in the boundary of $K \in \mathcal{M}$, it is

1. Notice that these “edges” are not necessarily “true” edges of the control volumes: a true edge of a control volume can sometimes be cut into several edges of the discretization.

assumed that $\partial K = \cup_{\sigma \in \mathcal{E}_K} \sigma$. It is also required that each edge σ is either shared by two different control volumes K and L (in which case σ is called an interior edge and we sometimes write $\sigma^{K,L}$ to indicate that K and L are the control volumes on either side of σ) or is included in $\partial\Omega$ (in which case σ is called an exterior edge and we sometimes write $\sigma^{K,\partial}$ to indicate that K is the unique control volume containing σ in its boundary). The set of interior and exterior edges are respectively denoted by \mathcal{E}_{int} and \mathcal{E}_{ext} .

Each method also demands special admissibility assumptions on the discretization, and probably other elements of discretization (such as points inside the control volumes, etc.); these precise assumptions and additional elements will not be useful to us (we simply consider that, if a specific method has been chosen, this means that the discretization is admissible with respect to this method).

Unknowns: the unknowns associated with the finite volume scheme are:

- approximate values $(u_K)_{K \in \mathcal{M}}$ of the solution in the control volumes,
- approximate values $(u_\sigma)_{\sigma \in \mathcal{E}_{\text{ext}}}$ of the solution on the edges contained in $\partial\Omega$,
- approximate values $(F_{K,\sigma})_{K \in \mathcal{M}, \sigma \in \mathcal{E}_K}$ of the fluxes $\int_\sigma A \nabla u \cdot \mathbf{n}_{K,\sigma}$ ($\mathbf{n}_{K,\sigma}$ is the normal to σ outward K).

Notice that some schemes necessitate the introduction of more unknowns, which we then call *dummy unknowns*; others can reduce the number of unknowns, expressing the fluxes by means of the approximate values in each control volume. These specificities will be of no interest to us: we only require that the preceding unknowns $(u_K, u_\sigma, F_{K,\sigma})$ exist or can be reconstructed in the considered schemes, and that they satisfy the following basic equations.

Basic relations: the basic physical laws that lead to [1]–[2] are:

$$\forall \sigma^{K,L} \in \mathcal{E}_{\text{int}}, \quad F_{K,\sigma} + F_{L,\sigma} = 0 \quad (\text{conservativity of the fluxes}), \quad [3]$$

$$\forall K \in \mathcal{M}, \quad - \sum_{\sigma \in \mathcal{E}_K} F_{K,\sigma} = m(K) f_K \quad (\text{balance of the fluxes}), \quad [4]$$

$$\forall \sigma \in \mathcal{E}_{\text{ext}}, \quad u_\sigma = g_\sigma \quad (\text{boundary conditions}), \quad [5]$$

where $m(K)$ is the measure of the control volume K and f_K and g_σ are appropriate approximate values of f and g on K and σ (the most common choices are the mean values on K and σ , which we assume in the following).

There are additional equations (needed to obtain a square linear system), which define each specific finite volume method. As for the discretization of Ω and the set of unknowns, these additional elements will be of no use to us, as we intend to rely only on global approximation properties of the schemes (see section 4).

From now on, all the schemes we consider are based on the preceding core elements and we use the following notations.

Notations: ω being a polygonal open domain of \mathbb{R}^d , a *FV scheme* for [1]–[2] on ω is (S, \mathcal{D}) where S is a finite volume method for [1]–[2] on ω (i.e. a way, given an admissible discretization, to construct an approximation of the solution to [1]–[2] on ω) and $\mathcal{D} = (\mathcal{M}, \mathcal{E})$ is an admissible (with respect to this method) discretization of ω . What we call a solution U to (S, \mathcal{D}) is in fact the extraction of all non-dummy unknowns of a complete solution to the scheme: $U = ((u_K)_{K \in \mathcal{M}}, (u_\sigma)_{\sigma \in \mathcal{E}_{\text{ext}}}, (F_{K,\sigma})_{K \in \mathcal{M}, \sigma \in \mathcal{E}_K})$. We denote by $u : \Omega \rightarrow \mathbb{R}$ the piecewise constant function equal to u_K on the control volume $K \in \mathcal{M}$ and by $t(U) : \partial\omega \rightarrow \mathbb{R}$ the piecewise constant function equal to u_σ on the edge $\sigma \in \mathcal{E}_{\text{ext}}$. When U is equipped with an index or an exponent (say U^b or U_n), the same notation is transferred to u (which gives u^b or u_n), but not necessarily to u_K , u_σ or $F_{K,\sigma}$ in order to keep the notations light (the situation makes it clear when these scalar data correspond to a U_n or a u^b , for example).

3. How should two finite volume schemes be coupled?

We now consider the situation where Ω is cut into two connected polygonal domains Ω^b and Ω^\sharp , and we denote by $\Gamma = \partial\Omega^b \cap \Omega = \partial\Omega^\sharp \cap \Omega = \partial\Omega^b \cap \partial\Omega^\sharp$ their interface. We assume that each region Ω^b and Ω^\sharp has been discretized in such a way that these discretizations $\mathcal{D}^b = (\mathcal{M}^b, \mathcal{E}^b)$ and $\mathcal{D}^\sharp = (\mathcal{M}^\sharp, \mathcal{E}^\sharp)$ are compatible on Γ : each exterior edge of each discretization is either completely included in Γ or does not intersect Γ , and each edge of $\mathcal{E}_{\text{ext}}^b$ contained in Γ is also an edge of $\mathcal{E}_{\text{ext}}^\sharp$ (and vice-versa); see Figure 1 (in which certain “geometrical” edges are in fact cut into two edges of discretization).

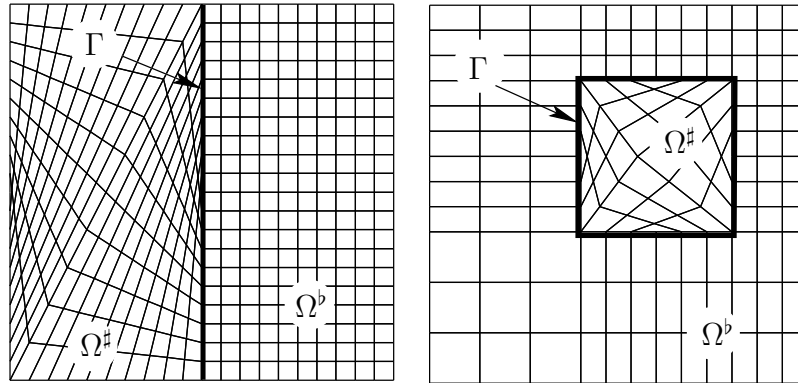


Figure 1. Examples of Ω cut into Ω^b and Ω^\sharp , with discretizations of each subdomain.

We want to approximate the solution to [1]–[2] using one finite volume method S^b in Ω^b , on the discretization \mathcal{D}^b , and another finite volume method S^\sharp in Ω^\sharp , on the discretization \mathcal{D}^\sharp . Assuming that these discretizations are admissible with respect to the corresponding methods, it is straightforward to write most of the equations of S^b

and S^\sharp in each subdomain, including the boundary conditions $u = g$ on $\partial\Omega^b \cap \partial\Omega = \partial\Omega^b \setminus \Gamma$ and $\partial\Omega^\sharp \cap \partial\Omega = \partial\Omega^\sharp \setminus \Gamma$. The only equations of S^b and S^\sharp which we cannot write are the ones concerning the boundary conditions on Γ , that is to say, for each scheme, equations [5] for $\sigma \subset \Gamma$ (notice that Γ is a piece of the boundaries of the domains Ω^b and Ω^\sharp , on which we use S^b and S^\sharp). Hence, to close the global linear system, there lacks as many equations as twice the number of edges contained in Γ (once this number for each scheme).

The equations we must add to those of S^b and S^\sharp already written are in fact quite obvious: we do not want the approximate solution to have a jump across Γ (because the continuous one does not), and the fluxes should remain conservative across this interface. Denoting with a superscript b and $^\sharp$ unknowns respectively corresponding to S^b and S^\sharp , the additional equations therefore are:

$$\text{for all edge } \sigma \subset \Gamma, \quad u_\sigma^b = u_\sigma^\sharp, \quad [6]$$

$$\begin{aligned} &\text{for all edge } \sigma \subset \Gamma, \text{ denoting by } K \in \mathcal{M}^b \text{ and } L \in \mathcal{M}^\sharp \\ &\text{the control volumes on each side of } \sigma, \quad F_{K,\sigma}^b + F_{L,\sigma}^\sharp = 0. \end{aligned} \quad [7]$$

This gives the desired number of supplemental equations, and the linear system consisting of the equations of S^b in Ω^b , the equations of S^\sharp in Ω^\sharp , [6] and [7] is therefore square. The scheme thus obtained is denoted by S^b - S^\sharp -[6]-[7].

4. What can ensure that such a coupling works?

In this section, we try and find properties that are usually satisfied by finite volume schemes and that ensure, if separately verified by S^b and S^\sharp , that the coupling S^b - S^\sharp -[6]-[7] has a unique approximate solution which converges, as the size of the discretizations tend to 0, to the solution of [1]-[2].

4.1. Solvability

The existence of a solution to a finite volume scheme is often linked to *a priori* estimates involving a so-called “discrete H^1 -norm” associated with the scheme.

Definition 1 (Property N) *A FV scheme (S, \mathcal{D}) for [1]-[2] on ω satisfies Property N if, for any solution $U = ((u_K)_{K \in \mathcal{M}}, (u_\sigma)_{\sigma \in \mathcal{E}_{\text{ext}}}, (F_{K,\sigma})_{K \in \mathcal{M}, \sigma \in \mathcal{E}_K})$ to (S, \mathcal{D}) , the quantity*

$$|U|_{S,\mathcal{D}}^2 = \sum_{\sigma^{K,L} \in \mathcal{E}_{\text{int}}} F_{K,\sigma}(u_L - u_K) + \sum_{\sigma^{K,\partial} \in \mathcal{E}_{\text{ext}}} F_{K,\sigma}(u_\sigma - u_K) \quad [8]$$

is indeed positive, and if all the unknowns of S are zero as soon as $|U|_{S,\mathcal{D}}$ and one of the $(u_\sigma)_{\sigma \in \mathcal{E}_{\text{ext}}}$ are zero.

Theorem 1 *If (S^b, \mathcal{D}^b) and $(S^\sharp, \mathcal{D}^\sharp)$ both satisfy Property N, then the scheme S^b – S^\sharp –[6]–[7] has one and only one solution.*

Sketch of proof of Theorem 1

For each scheme $i \in \{b, \sharp\}$, we multiply [4] by the corresponding unknown u_K^i , sum on the control volumes $K \in \mathcal{M}^i$ and use the conservativity [3] to gather the sums by edges. Summing on $i = b, \sharp$ and taking into account [5], [6] and [7], this leads to

$$\sum_{i=b, \sharp} \sum_{K \in \mathcal{M}^i} m(K) f_K u_K^i + \sum_{i=b, \sharp} \sum_{\substack{\sigma^{K, \partial} \in \mathcal{E}_{\text{ext}}^i \\ \sigma \subset \partial\Omega^i \setminus \Gamma}} F_{K, \sigma}^i g_\sigma = |U^b|_{S^b, \mathcal{D}^b}^2 + |U^\sharp|_{S^\sharp, \mathcal{D}^\sharp}^2. \quad [9]$$

Thus, if the right-hand side (f, g) of the system vanishes, so does $|U^b|_{S^b, \mathcal{D}^b}$ and $|U^\sharp|_{S^\sharp, \mathcal{D}^\sharp}$. Since at least one of the two subdomains sees $\partial\Omega$, where the boundary condition g is zero, Property N implies that, in this subdomain, all the unknowns vanish, which extends to the other subdomain through the equality of the boundary unknowns on Γ . Hence, the linear square system S^b – S^\sharp –[6]–[7] is solvable. ■

4.2. A priori estimates

To simplify the rest of the presentation, we assume from now on that $g = 0$ (which, because of Γ , does not mean that the schemes S^b and S^\sharp are only written with homogeneous Dirichlet conditions).

Quantity [8] used to prove the solvability of the scheme is also well suited to obtaining estimates: from [9] we notice that

$$|U^b|_{S^b, \mathcal{D}^b}^2 + |U^\sharp|_{S^\sharp, \mathcal{D}^\sharp}^2 \leq \|f\|_{L^2(\Omega)} \left(\|u^b\|_{L^2(\Omega^b)} + \|u^\sharp\|_{L^2(\Omega^\sharp)} \right). \quad [10]$$

If both subdomains Ω^b and Ω^\sharp see enough of $\partial\Omega$ (as in the first example in Figure 1), then both schemes S^b and S^\sharp make use of homogeneous Dirichlet conditions on a large part of the boundary and we can expect the existence of Poincaré's inequalities, i.e. that the L^2 norms of u^b and u^\sharp are controlled by $|U^b|_{S^b, \mathcal{D}^b}$ and $|U^\sharp|_{S^\sharp, \mathcal{D}^\sharp}$: this is the situation depicted by Property P₀ below (in which Λ is intended to play the role of $\partial\Omega^b \setminus \Gamma$ or $\partial\Omega^\sharp \setminus \Gamma$). However it can happen that one of the domains does not see (enough of) the boundary of $\partial\Omega$, in which case the second sees all (or nearly all) of it: that is the case in the second example of Figure 1. Assume that it happens to Ω^\sharp ; in this situation, the best we can hope for is to estimate $\|u^\sharp\|_{L^2(\Omega^\sharp)}$ by means of $|U^\sharp|_{S^\sharp, \mathcal{D}^\sharp}$ and $\|t(U^\sharp)\|_{L^2(\partial\Omega^\sharp)}$ (Property P below); to bound $t(U^\sharp)$, which is zero outside Γ , we then use [6], which states that $t(U^\sharp) = t(U^b)$ on Γ , and the fact that $t(U^b)$ can probably be controlled by $|U^b|_{S^b, \mathcal{D}^b}$ since Ω^b sees $\partial\Omega$ (cf. Property T below).

Definition 2 (Properties P₀ and P) *Let $(S, \mathcal{D}_n)_{n \geq 1}$ be FV schemes for [1]–[2] on ω and let $\Lambda \subset \partial\omega$. Then $(S, (\mathcal{D}_n)_{n \geq 1}, \Lambda)$ satisfies Property P₀ or Property P if there*

exists $C > 0$ such that, for all $n \geq 1$ and any solution U of (S, \mathcal{D}_n) satisfying $u_\sigma = 0$ whenever $\sigma \subset \Lambda$, the corresponding inequality holds:

$$\|u\|_{L^2(\omega)} \leq C|U|_{S, \mathcal{D}} \quad (\text{for Property } P_0),$$

$$\|u\|_{L^2(\omega)} \leq C (\|t(U)\|_{L^2(\partial\omega)} + |U|_{S, \mathcal{D}}) \quad (\text{for Property } P).$$

Definition 3 (Property T) Let $(S, \mathcal{D}_n)_{n \geq 1}$ be FV schemes for [1]–[2] on ω and let $\Lambda \subset \partial\omega$. Then $(S, (\mathcal{D}_n)_{n \geq 1}, \Lambda)$ satisfies Property T if there exists $C > 0$ such that, for all $n \geq 1$ and any solution U of (S, \mathcal{D}_n) satisfying $u_\sigma = 0$ whenever $\sigma \subset \Lambda$, we have $\|t(U)\|_{L^2(\partial\omega)} \leq C (\|u\|_{L^2(\omega)} + |U|_{S, \mathcal{D}})$.

REMARK. — In general, Properties P and T are verified even for functions which do not vanish on Λ .

The *a priori* estimates we can then obtain are described in the following theorem.

Theorem 2 Let $(\mathcal{D}_n^b)_{n \geq 1}$ and $(\mathcal{D}_n^\sharp)_{n \geq 1}$ be discretizations of Ω^b and Ω^\sharp such that, for all $n \geq 1$, (S^b, \mathcal{D}_n^b) and $(S^\sharp, \mathcal{D}_n^\sharp)$ satisfy Property N. Assume that $(S^b, (\mathcal{D}_n^b)_{n \geq 1}, \partial\Omega^b \setminus \Gamma)$ satisfies Property P_0 and that either one of the following holds:

1) $(S^\sharp, (\mathcal{D}_n^\sharp)_{n \geq 1}, \partial\Omega^\sharp \setminus \Gamma)$ satisfies Property P_0 , or

2) $(S^\sharp, (\mathcal{D}_n^\sharp)_{n \geq 1}, \partial\Omega^\sharp \setminus \Gamma)$ satisfies Property P and $(S^b, (\mathcal{D}_n^b)_{n \geq 1}, \partial\Omega^b \setminus \Gamma)$ satisfies Property T.

Then there exists C_1 such that, for all $n \geq 1$, if (U_n^b, U_n^\sharp) is the solution to S^b – S^\sharp –[6]–[7] on $(\mathcal{D}_n^b, \mathcal{D}_n^\sharp)$,

$$\|u_n^b\|_{L^2(\Omega^b)} + |U_n^b|_{S^b, \mathcal{D}_n^b} + \|u_n^\sharp\|_{L^2(\Omega^\sharp)} + |U_n^\sharp|_{S^\sharp, \mathcal{D}_n^\sharp} \leq C_1.$$

Sketch of proof of Theorem 2

We have $\|u_n^b\|_{L^2(\Omega^b)} \leq C_2 |U_n^b|_{S^b, \mathcal{D}_n^b}$. In either case 1) or 2), relying on the general reasoning described above, we can see that $\|u_n^\sharp\|_{L^2(\Omega^\sharp)} \leq C_3 (|U_n^b|_{S^b, \mathcal{D}_n^b} + |U_n^\sharp|_{S^\sharp, \mathcal{D}_n^\sharp})$. Using [10], we then deduce the estimate on U_n^b and U_n^\sharp which, in turn, give the bound on u_n^b and u_n^\sharp . ■

4.3. Convergence

The usual proof of convergence in finite volume methods is achieved in two steps: first, it is shown that the *a priori* estimates involving the $|\cdot|_{S, \mathcal{D}}$ norm give some compactness properties on the approximate solutions, which makes it possible to extract a subsequence converging toward a function of H^1 (this is translated in Property C below); then, it is shown that the subsequent limit is the weak solution to the PDE (this is the purpose of Property L below); in particular, this proves that there can only be one

limit for subsequences of approximate solutions, and hence that the whole sequence converges.

Definition 4 (Property C) Let $(S, \mathcal{D}_n)_{n \geq 1}$ be FV schemes for [1]–[2] on ω such that the size of \mathcal{D}_n (²) tends to 0 as $n \rightarrow \infty$, and let $\Lambda \subset \partial\omega$. We say that $(S, (\mathcal{D}_n)_{n \geq 1}, \Lambda)$ satisfies Property C if, for all solution U_n of (S, \mathcal{D}_n) such that $u_\sigma = 0$ whenever $\sigma \subset \Lambda$ and $(\|u_n\|_{L^2(\omega)} + |U_n|_{S, \mathcal{D}_n})_{n \geq 1}$ is bounded, up to a subsequence, $(u_n)_{n \geq 1}$ converges weakly-* in $L^2(\omega)$ to some $\bar{u} \in H^1(\omega)$ and $t(U_n) \rightarrow \gamma(\bar{u})$ weakly-* in $L^2(\partial\omega)$ (where γ is the usual trace operator on $H^1(\omega)$).

REMARK. — All finite volume methods achieve a much better convergence than this weak-* convergence: this convergence holds in general in $L^2(\omega)$, or even better.

Definition 5 (Property L) Let $(S, \mathcal{D}_n)_{n \geq 1}$ be FV schemes for [1]–[2] on ω such that the size of \mathcal{D}_n tends to 0 as $n \rightarrow \infty$, and let $\Gamma \subset \partial\omega$. Let $I_n : C^\infty(\mathbb{R}^d) \rightarrow L^2(\Gamma)$ be a projector on the piecewise constant functions adapted to $\mathcal{E}_{n, \text{ext}}$: $I_n(\varphi) = (I_n(\varphi)_\sigma)_{\sigma \in \mathcal{E}_{n, \text{ext}}, \sigma \subset \Gamma}$. We say that $(S, (\mathcal{D}_n)_{n \geq 1}, \Gamma, (I_n)_{n \geq 1})$ satisfies Property L if, for any U_n solution of (S, \mathcal{D}_n) such that $(|U_n|_{S, \mathcal{D}_n})_{n \geq 1}$ is bounded and $(u_n)_{n \geq 1}$ converges weakly-* in $L^2(\omega)$ to some $\bar{u} \in H^1(\omega)$, for all $\varphi \in C^\infty(\mathbb{R}^d)$ the support of which does not intersect $\partial\omega \setminus \Gamma$, there exists piecewise constant functions $\varphi_{\mathcal{M}_n} = (\varphi_K)_{K \in \mathcal{M}_n}$ which converge to φ weakly-* in $L^2(\omega)$ as $n \rightarrow \infty$, such that $\varphi_K = 0$ whenever $\text{supp}(\varphi) \cap K = \emptyset$ and, as $n \rightarrow \infty$,

$$\sum_{\sigma^{K,L} \in \mathcal{E}_{n, \text{int}}} F_{K, \sigma}(\varphi_L - \varphi_K) + \sum_{\substack{\sigma^{K, \partial} \in \mathcal{E}_{n, \text{ext}} \\ \sigma \subset \Gamma}} F_{K, \sigma}(I_n(\varphi)_\sigma - \varphi_K) \rightarrow \int_{\omega} A \nabla \bar{u} \cdot \nabla \varphi. \quad [11]$$

REMARK. — The terms $\varphi_L - \varphi_K$ and $I_n(\varphi)_\sigma - \varphi_K$ approximate the fluxes of $\nabla \varphi$ and, assuming that $A = \text{Id}$ to simplify the reasoning, finite volume schemes are usually built so that a discrete integration by parts in the left-hand side of [11] leads to $-\int_{\omega} u_n \Delta \varphi + \int_{\partial\omega} t(U_n) \nabla \varphi \cdot \mathbf{n} + \alpha_n$ with $\lim_{n \rightarrow \infty} \alpha_n = 0$ (³); passing to the limit thanks to Property C, this gives $-\int_{\omega} \bar{u} \Delta \varphi + \int_{\partial\omega} \gamma(\bar{u}) \nabla \varphi \cdot \mathbf{n} = \int_{\omega} \nabla \bar{u} \cdot \nabla \varphi$ and Property L is thus quite natural.

Let us now state the convergence result concerning $S^{\flat} - S^{\sharp}$ –[6]–[7].

Theorem 3 Assume the assumptions of Theorem 2 and that $(S^{\flat}, (\mathcal{D}_n^{\flat})_{n \geq 1}, \partial\Omega^{\flat} \setminus \Gamma)$ and $(S^{\sharp}, (\mathcal{D}_n^{\sharp})_{n \geq 1}, \partial\Omega^{\sharp} \setminus \Gamma)$ satisfy Property C. We also assume that there exists projectors $I_n : C^\infty(\mathbb{R}^d) \rightarrow L^2(\Gamma)$ on the piecewise constant functions adapted to $\mathcal{E}_{n, \text{ext}}^{\flat}$ (⁴) such that $(S^{\flat}, (\mathcal{D}_n^{\flat})_{n \geq 1}, \Gamma, (I_n)_{n \geq 1})$ and $(S^{\sharp}, (\mathcal{D}_n^{\sharp})_{n \geq 1}, \Gamma, (I_n)_{n \geq 1})$ satisfy Property L. Let $(U_n^{\flat}, U_n^{\sharp})$ be the solution to $S^{\flat} - S^{\sharp}$ –[6]–[7] and let u_n be equal to u_n^{\flat} on Ω^{\flat}

2. That is to say the maximum of the diameters of the control volumes of \mathcal{D}_n .
3. Or sometimes even directly $\int_{\omega} (\nabla u)_n \cdot \nabla \varphi + \alpha_n$, if an approximate value $(\nabla u)_n$ of the gradient of the solution is provided by the scheme.
4. And thus also to $\mathcal{E}_{n, \text{ext}}^{\sharp}$.

and to u_n^\sharp on Ω^\sharp . Then $(u_n)_{n \geq 1}$ converges to the weak solution of [1]–[2] weakly-* in $L^2(\Omega)$, and in any Lebesgue space in which the convergence in Property C holds for S^b and S^\sharp .

Sketch of proof of Theorem 3

From Theorem 2 and Property C we have, up to a subsequence, $u_n^b \rightarrow \bar{u}^b$ and $u_n^\sharp \rightarrow \bar{u}^\sharp$ weakly-* in $L^2(\Omega^b)$ and $L^2(\Omega^\sharp)$, where $\bar{u}^b \in H^1(\Omega^b)$ and $\bar{u}^\sharp \in H^1(\Omega^\sharp)$. Since the traces $t(U_n^b)$ and $t(U_n^\sharp)$ weakly-* converge to the traces of \bar{u}^b and \bar{u}^\sharp , the homogeneous Dirichlet boundary conditions and equality [6] of these traces on Γ ensure that the function \bar{u} equal to \bar{u}^b on Ω^b and to \bar{u}^\sharp on Ω^\sharp belongs to $H_0^1(\Omega)$.

It remains to prove that \bar{u} is the weak solution to [1]–[2] (with $g = 0$). Let $\varphi \in C_c^\infty(\Omega)$; for each $i \in \{b, \sharp\}$, we multiply equation [4] of the scheme S^i by φ_K^i (from the piecewise approximation $\varphi_{\mathcal{M}_n^i}$ of φ given by Property L of S^i), sum on K and use the conservativity [3] to gather by edges, eliminating from this sum the edges on $\partial\Omega$ since φ vanishes near this boundary. From [7] we have, for all $\sigma^{K,L} \subset \Gamma$, $F_{K,\sigma}^b I_n(\varphi)_\sigma + F_{L,\sigma}^\sharp I_n(\varphi)_\sigma = 0$; this allows us to introduce $I_n(\varphi)_\sigma$ into the preceding results so that, when we sum them on $i = b, \sharp$, we find

$$\begin{aligned} \sum_{i=b,\sharp} \left(\sum_{\sigma^{K,L} \in \mathcal{E}_{n,\text{int}}^i} F_{K,\sigma}^i (\varphi_L^i - \varphi_K^i) + \sum_{\substack{\sigma^{K,\partial} \in \mathcal{E}_{n,\text{ext}}^i \\ \sigma \subset \Gamma}} F_{K,\sigma}^i (I_n(\varphi)_\sigma - \varphi_K^i) \right) \\ = \sum_{i=b,\sharp} \int_{\Omega^i} f \varphi_{\mathcal{M}_n^i}. \end{aligned}$$

Property L of both schemes then shows, passing to the limit $n \rightarrow +\infty$, that \bar{u} satisfies the weak formulation of [1]–[2]. ■

REMARK. — As the proof shows, it is important that the discretization of φ on Γ (via $I_n(\varphi)$) is the same for both schemes, which may require additional compatibility assumptions on \mathcal{D}^b and \mathcal{D}^\sharp on Γ .

5. Implementation and numerical results

5.1. A word on practical implementation

Although the objectives of the presentation above are not the same as those of domain decomposition techniques, there are of course formal similarities between the two theories. In particular, we can try and solve S^b – S^\sharp –[6]–[7] via iterative methods, using only pre-existing separate codes for S^b and S^\sharp . Let $\mathcal{F}(\Gamma)$ be the set of functions on Γ which are constant on each edge $\sigma \subset \Gamma$ and, for $i = b, \sharp$, define the Dirichlet-to-Neumann operator $T^i : \mathcal{F}(\Gamma) \rightarrow \mathcal{F}(\Gamma)$ in domain Ω^i : $T^i(X) = (\frac{1}{m(\sigma)} F_{K,\sigma}^i)_{\sigma \subset \Gamma}$, where $U^i = ((u_K)_{K \in \mathcal{M}^i}, (u_\sigma)_{\sigma \in \mathcal{E}_{\text{ext}}^i}, (F_{K,\sigma})_{K \in \mathcal{M}^i, \sigma \in \mathcal{E}_K})$ is the solution to (S^i, \mathcal{D}^i) with $f = 0$ and boundary condition equal to 0 on $\partial\Omega^i \setminus \Gamma$ and to

X on Γ . In view of [6] and [7], computing the solution to the coupling of S^b and S^\sharp comes down to solving an equation $T^b(X) + T^\sharp(X) = H$ (where H takes into account the right-hand side f). Using the L^2 scalar product on $\mathcal{F}(\Gamma)$, it is easy to see that

$$\langle T^i(X), Y \rangle = \sum_{\sigma^{K,L} \in \mathcal{E}_{\text{int}}^i} F_{K,\sigma}(v_L - v_K) + \sum_{\sigma \in \mathcal{E}_{\text{ext}}^i} F_{K,\sigma}(v_\sigma - v_K) \quad [12]$$

where $((v_K)_{K \in \mathcal{M}^i}, (v_\sigma)_{\sigma \in \mathcal{E}_{\text{ext}}^i}, (G_{K,\sigma})_{K \in \mathcal{M}^i, \sigma \in \mathcal{E}_K})$ is the solution to (S^i, \mathcal{D}^i) corresponding to boundary condition Y on Γ (indeed, since $(F_{K,\sigma})_{\sigma \in \mathcal{E}_K}$ satisfies [4] with $f = 0$, the terms involving v_K and v_L in [12] vanish). For most schemes, the right-hand side of [12] is a discrete equivalent of $\int_\omega A \nabla u \cdot \nabla v$ and, therefore, if A is symmetric we can expect T^i to also be symmetric. Moreover, $\langle T^i(X), X \rangle = |U|_{S^i, \mathcal{D}^i}^2$ is non-negative and, for at least one $i = b, \sharp$ (such that S^i satisfies Property P_0), say $i = b$, in virtue of Property T, we have $\langle T^i(X), X \rangle \geq C \|X\|^2$. Operators T^b and T^\sharp both being continuous (the dimension of $\mathcal{F}(\Gamma)$ is finite), we can therefore invoke [QUA 99, Theorem 4.2.2] to ensure that, for some $\theta > 0$ small enough, the iterative method $X_{k+1} = X_k + \theta(T^b)^{-1}(H - T^b(X_k) - T^\sharp(X_k))$ converges to the solution X of $T^b(X) + T^\sharp(X) = H$.

This iterative procedure can be implemented by separately solving S^b and S^\sharp (alternatively with Dirichlet and Neumann boundary conditions for S^b), and is therefore agreeable if codes for each scheme are already available. However, fixing a θ ensuring the convergence of the iterations and estimating the corresponding rate demands to delve into the specificities of each scheme (to compute coercivity and continuity constants of T^b and T^\sharp). In the following numerical tests, we therefore preferred to implement a specific code to directly solve S^b - S^\sharp -[6]-[7].

5.2. Framework of the numerical tests

We present one example of the coupling of two finite volume schemes: the standard 2-point finite volume scheme from [EYM 00] and the mixed finite volume scheme from [DRO 06-2]. The standard 2-point finite volume scheme (denoted by ‘‘FV2’’ below) has only one unknown u_K per control volume K , but requires the grid to have strong orthogonal properties. The mixed finite volume scheme (denoted by ‘‘MFV’’ below) is written with many more unknowns (the basic unknowns from section 2 and approximate values of the gradient in each control volume); fortunately, a hybridization method makes it possible to write it using only one unknown per edge (approximate values of the solution on the edges), which is nevertheless more expensive than the 2-point finite volume scheme. On the other hand, it can be used on nearly any grid (in dimension 2 or more), and for a wide class of equations (from anisotropic heterogeneous linear ones [DRO 06-2], to fully non-linear equations of the p -laplacian type [DRO 06-1], to miscible flows in porous media [CHA 07], to Navier-Stokes equations [DRO 07]). In a forthcoming work, we will prove that both FV2 and MFV satisfy all the properties N, P_0 , P, T, C and L stated in section 4 (with, of course, an adapted choice of Λ for Property P_0).

Each grid admissible for the coupling of the two preceding schemes is also admissible for the pure MFV. As explained in the introduction, the aim of the coupling method is to reduce the cost of the scheme by applying, where possible, the simpler 2-point finite volume scheme instead of the mixed finite volume scheme. In the case of the coupling of FV2 and MFV, the method is therefore efficient if it leads to a significant reduction in the size of the system (with respect to the pure MFV), while preserving the error between the approximate and exact solutions, and the qualitative properties of the approximate solution.

We denote, for a given test, the number of control volumes by NCV, the number of unknowns by UNK, the L^2 relative error by e_2 and the L^∞ relative error by e_∞ (relative errors are the errors divided by the norm of the solution). The linear systems are solved using direct Gauss eliminations. In a first batch of tests, we concentrate on the behaviour of the coupling method with respect to various griddings of the domain, and not on the influence of anisotropy or heterogeneity phenomena. In a second series of tests, we study the ability of the method to handle strong heterogeneities in the diffusion tensor, which in particular lead to an irregular right-hand side.

5.3. Effect of various griddings of the domain

We take here $\Omega =]0, 1[^2$ and $A = \text{Id}$. The source term f is chosen so that the exact solution is $\bar{u}(x, y) = x(1-x)y(1-y)$.

The first test we consider involves cartesian grids. On such grids, we can apply either FV2, MFV or the coupling of both schemes (using for example FV2 on $\Omega^b = \{x > 0.5\}$ and MFV on $\Omega^\sharp = \{x < 0.5\}$). We compare those three choices in Table 1. Of course, for such a grid, it is unwise to use a complex scheme such as the MFV or even the coupling of MFV and FV2; we only present those results to show that they all lead to similar errors (and a convergence of order roughly 2 with respect to the size of the mesh).

The second test is based on a family of grids constructed from the first example of Figure 1, by uniform subdivisions of each control volume. The subdomain $\Omega^\sharp = \{x < 0.5\}$ is not admissible with respect to FV2, so we use FVM on it; on the contrary, the subdomain $\Omega^b = \{x > 0.5\}$ is adapted to FV2 and, in the coupling, we therefore use this simpler scheme on this domain. The results, given in Table 2, clearly show no degradation (and even an improvement) of the rates of convergence (roughly 2) between MFV and the coupling MFV-FV2, while in the meantime the coupling allows for an economy of nearly 25% on the number of unknowns. Moreover, as we can see in Figure 2 (which shows the grid and the solution to the coupling MFV-FV2 in the NCV=1600 case), the exchange of information between MFV and FV2 at the interface $\Gamma = \{x = 0.5\}$ provokes no perceptible perturbation of the approximate solution.

In all the preceding tests, both subdomains Ω^b and Ω^\sharp have a common boundary with the whole domain Ω (and hence both schemes applied on these subdomains satisfy Property P₀); let us now consider a case where Ω^\sharp is completely inside Ω , and

		FV2			
NCV	UNK	e_2	e_∞		
6400	6400	2.29E-4	1.54E-4		
10000	10000	1.46E-4	9.93E-5		
22500	22500	6.52E-5	4.42E-5		
40000	40000	3.67E-5	2.49E-5		

		MFV			Coupling MFV-FV2		
NCV	UNK	e_2	e_∞	UNK	e_2	e_∞	
6400	12640	2.29E-4	1.55E-4	9560	2.21E-4	1.55E-4	
10000	19800	1.47E-4	9.93E-5	14950	1.41E-4	9.95E-5	
22500	44700	6.47E-5	4.42E-5	33675	6.27E-5	4.42E-5	
40000	79600	3.68E-5	2.49E-5	59900	3.56E-5	2.68E-5	

Table 1. Comparison between FV2, MFV and the coupling of both, on cartesian grids.

		MFV			Coupling MFV-FV2		
NCV	UNK	e_2	e_∞	UNK	e_2	e_∞	
10000	19800	2.97E-4	6.92E-4	14950	2.80E-4	6.93E-4	
22500	44700	1.32E-4	3.22E-4	33675	1.24E-4	3.22E-4	
40000	79600	7.39E-5	1.85E-4	59900	7.03E-5	1.85E-4	

Table 2. Comparison between MFV and the coupling MFV-FV2, on grids constructed from the pattern in Figure 2.

thus the scheme applied on this subdomain satisfies only Property P. The grids we use are constructed by uniform subdivision of the second example in Figure 1 and, obviously, we use MFV on Ω^\sharp (not admissible for FV2) and FV2 on Ω^b . The results are presented in Table 3, and one grid and solution are drawn in Figure 3. As before, the pure MFV and the coupling MFV-FV2 lead to errors of similar magnitude, and the coupling provokes no numerical glitch around the interface Γ between the two subdomains. The gain on the number of unknowns is even greater here (more than 33%).

		MFV			Coupling MFV-FV2		
NCV	UNK	e_2	e_∞	UNK	e_2	e_∞	
10000	19800	2.75E-4	3.38E-4	12600	2.92E-4	3.37E-4	
21904	43512	1.25E-4	1.54E-4	29032	1.26E-4	1.49E-4	
40000	79600	6.98E-5	8.63E-5	50200	7.31E-5	8.99E-5	

Table 3. Comparison between MFV and the coupling MFV-FV2, on grids constructed from the pattern in Figure 3.

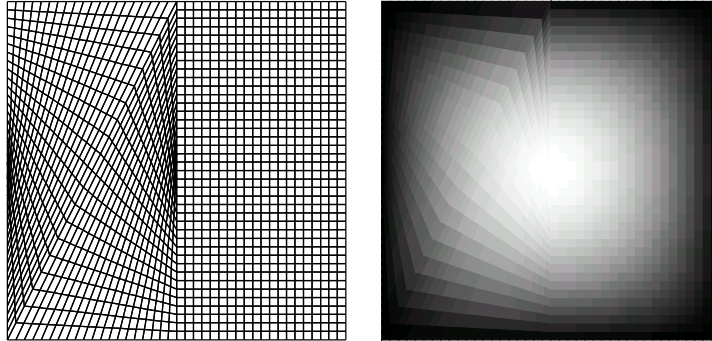


Figure 2. Grid (1600 control volumes) and solution (white=max, black=min): MFV in $\{x < 0.5\}$ and FV2 in $\{x > 0.5\}$.

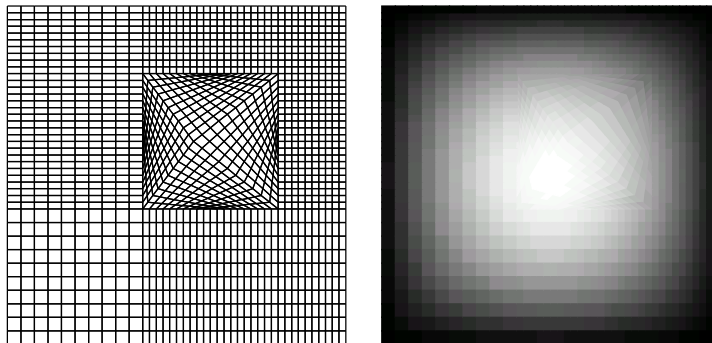


Figure 3. Grid (1600 control volumes) and solution (white=max, black=min): MFV in $]0.4, 0.8[^2$ and FV2 elsewhere.

In the last numerical test, we consider grids made of triangles instead of quadrangles; the general pattern is presented in Figure 4. The triangle formed by $(0, 0)$, $(0.5, 0.7)$ and $(1, 0)$ is discretized by an admissible FV2 grid (all triangular control volumes inside have acute angles), whereas we must use MFV on the rest of the domain. The results, presented in Table 4 and Figure 4, once again show similar errors for MFV and MFV-FV2 (less than 5% of difference on the relative errors), but the gain on the number of unknowns is much less significant than in the case of quadrangular meshes (around 8%).

NCV	MFV			Coupling MFV-FV2		
	UNK	e_2	e_∞	UNK	e_2	e_∞
10000	14900	5.76E-4	1.15E-3	13725	6.04E-4	1.15E-3
22500	33600	2.56E-4	5.12E-4	30900	2.68E-4	5.12E-4
40000	59800	1.44E-4	2.88E-4	54950	1.51E-4	2.88E-4

Table 4. Comparison between MFV and the coupling MFV-FV2, on grids constructed from the pattern in Figure 4.

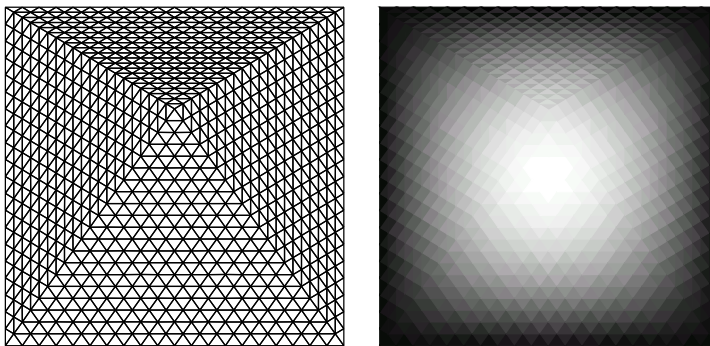


Figure 4. Grid (1600 control volumes) and solution (white=max, black=min): FV2 in the triangle $((0, 0), (0.5, 0.7), (1, 0))$ and MFV elsewhere.

5.4. Strong heterogeneity and irregular right-hand side

We still take $\Omega =]0, 1[^2$, but we now consider a heterogeneous discontinuous (though quite simple) diffusion tensor: $A(x, y) = k_l \text{Id}$ if $x \leq 0.5$ and $A(x, y) = k_r \text{Id}$ if $x > 0.5$, with k_l and k_r various positive constants. Since we are here interested in the effects of the discontinuity of the diffusion, we only consider a regular solution: $\bar{u}(x, y) = x^2$ (the boundary conditions are therefore no longer homogeneous). Notice that, in this case, the right-hand side $f = -\text{div}(A\nabla\bar{u})$ is not in $L^2(\Omega)$ but only in $(H^1(\Omega))'$: in fact, it is a measure with a singular part along the interface $\{x = 0.5\}$; its discretization $\int_K f$ is therefore not a real issue, except that it is necessary to choose, if $\{x = 0.5\}$ corresponds to edges of the grid, to which control volume (right or left) the singular part should be given (it can also be split between the two control volumes). We study here the impact of this choice.

We consider only two families of grids: cartesian grids and the family obtained by subdivisions of the grid in Figure 2. In both cases, we apply MFV on the domain $\{x \leq 0.5\}$ and FV2 on the domain $\{x > 0.5\}$, giving the singular part of the right-hand side to the control volumes in one domain or the other. The effect of the coupling

with respect to the reduction of the number of unknowns on these grids was studied above, so we only present the error results.

The results for the relative L^2 errors on cartesian grids are presented in Tables 5 (when the singular part of the right-hand side is given to the left domain, on which we apply MFV) and 6 (when the singular part of the right-hand side is given to the right domain, on which we apply FV2).

NCV	Ratio of the diffusions $\frac{k_r}{k_l}$				
	1E-4	1E-2	0	1E2	1E4
10000	3.47E-3	3.63E-3	4.32E-5	0.35	35.72
22500	2.23E-3	2.42E-3	1.92E-5	0.24	24.02
40000	1.62E-3	1.81E-3	1.07E-5	0.18	18.18

Table 5. Relative L^2 errors, with respect to the ratio of diffusions, for the coupling MFV-FV2 on cartesian grids; singular part of f given to the left (MFV) domain.

NCV	Ratio of the diffusions $\frac{k_r}{k_l}$				
	1E-4	1E-2	0	1E2	1E4
10000	36.90	0.36	4.32E-5	3.66E-3	3.73E-3
22500	24.60	0.24	1.92E-5	2.43E-3	2.48E-3
40000	18.46	0.18	1.07E-5	1.82E-3	1.85E-3

Table 6. Relative L^2 errors, with respect to the ratio of diffusions, for the coupling MFV-FV2 on cartesian grids; singular part of f given to the right (FV) domain.

Obviously, relative errors of order 0.2 or even 36 mean that the approximate solution has very little in common with the exact solution! However, we present these results because they allow for us to garner an interesting constatation.

We first notice that, in all the cases presented in Tables 5 and 6, even in the cases where the error is unacceptably large, the order of convergence is always 1 (except, of course, when there is no discontinuity of the diffusion tensor). This degradation, with respect to the order 2 noticed in the previous numerical tests, can be explained by the fact that the right-hand side f is singular here: it is only in $(H^1(\Omega))'$, not in $L^2(\Omega)$; the loss of one order of convergence is therefore compatible with the theoretical study and numerical observations in [DRO 03]. The next thing we notice, and probably the most important thing, is that the “constant” of the convergence (i.e. the C such that the error is bounded by C times the size of the mesh) strongly depend on the way we distribute the singular part of f ; if this singular part is given to the domain with strongest diffusion, C does not really vary with the ratio of the diffusions, and the results are therefore good even for strong diffusion ratios; on the other hand, if we put

the singular part of f in the domain with weakest diffusion ⁽⁵⁾, C varies linearly with respect to the diffusion ratio: hence, for “reasonable” sizes of meshes and large diffusion ratios, although the order of convergence is still 1, we obtain very bad L^2 errors. As the tables show, these results depend very little on the choice of the scheme (FV2 or MFV) used to discretize each domain, and in fact we noticed the same behaviour when applying only MFV or FV2 on the whole domain Ω .

We ran the same tests on grids obtained by subdivisions of that in Figure 2 (the results are presented in Tables 7 and 8 and in Figure 5); the order of convergence in this case is slightly less than 1, but the behaviour of the constant C is the same as for cartesian grids.

The general conclusion of these tests with highly heterogeneous diffusion is quite clear: the singular part of the right-hand side should always be given to the domain with the strongest diffusion. This should perhaps be linked to the usual handling of gravity forces in equations of the kind $-\text{div}(K(\nabla p - \rho g \nabla z)) = f$; when discretizing these equations, instead of considering $\text{div}(K(\rho g \nabla z))$ as a right-hand side to be integrated on the control volumes, this term is in general discretized by applying a finite volume scheme on z , which comes down to replacing $\int_K \text{div}(K(\rho g \nabla z))$ by the flux balance on K associated with this scheme. If a 2-point finite volume scheme is used, it is known by experience that, in the case of strong heterogeneity, the transmissivity coefficient on an edge should be calculated using a harmonic mean of the diffusions in the control volumes on each side; in this case, if $\sigma^{K,L}$ is an edge across which the diffusion tensor has a strong jump, and if K is in the region of strong diffusion and L in the region of weak diffusion, then all the transmissivities on the edges of L are small (of the order of the diffusion in L), whereas all the transmissivities on the edges of K except one, corresponding to σ , are large (of the order of the diffusion in K). Therefore, the right-hand side coming from the discretization of $\text{div}(K(\rho g \nabla z))$ is small on L and large on K and, although using a different means, this method comes down to handling the diffusion jump exactly as we advise above: put the singular part coming from this jump in the control volume where the diffusion is larger.

NCV	Ratio of the diffusions $\frac{k_r}{k_l}$				
	1E-4	1E-2	0	1E2	1E4
10000	4.40E-3	4.32E-3	3.38E-5	0.16	16.58
22500	2.96E-3	2.90E-3	1.50E-5	0.11	11.08
40000	2.23E-3	2.19E-3	8.46E-6	8.26E-2	8.32

Table 7. Relative L^2 errors, with respect to the ratio of diffusions, for the coupling MFV-FV2 on grids constructed from the grid in Figure 2; singular part of f given to the left (MFV) domain.

5. This is also the case if we split the singular part of f between the two domains.

NCV	Ratio of the diffusions $\frac{k_r}{k_l}$				
	1E-4	1E-2	0	1E2	1E4
10000	36.90	0.36	3.38E-5	3.64E-3	3.71E-3
22500	24.60	0.24	1.50E-5	2.42E-3	2.47E-3
40000	18.46	0.18	8.46E-6	1.81E-3	1.85E-3

Table 8. Relative L^2 errors, with respect to the ratio of diffusions, for the coupling MFV-FV2 on grids constructed from the grid in Figure 2; singular part of f given to the right (FV) domain.

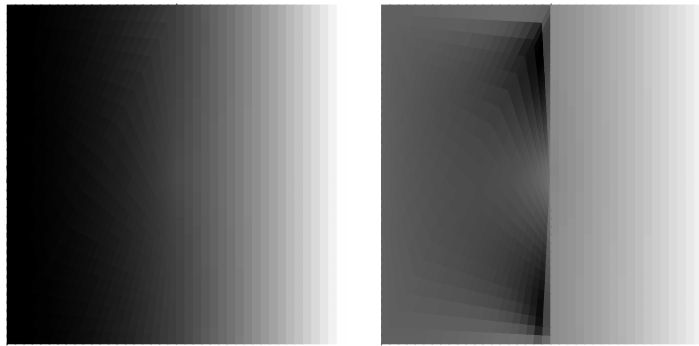


Figure 5. Approximate solution in the case of discontinuous diffusion; exact solution $\bar{u}(x, y) = x^2$; grid of Figure 2, singular part of the right-hand side given to the left (MFV) domain; ratios of diffusion $\frac{k_r}{k_l}$ equal to 10^{-2} (left) or 10^2 (right).

Acknowledgements

The author wishes to thank Robert Eymard for fruitful discussions and insights on FORTRAN programming.

6. References

- [AAV 98] AAVATSMARK I., BARKVE T., BOE O. AND MANNSETH, T., «Discretization on unstructured grids for inhomogeneous, anisotropic media. I. Derivation of the methods», *SIAM J. Sci. Comput.*, vol 19, n° 5, 1998, p. 1700–1716.
- [CHA 07] CHAINAIS-HILLAIRET C. AND DRONIOU J., «Convergence analysis of a mixed finite volume scheme for an elliptic-parabolic system modeling miscible fluid flows in porous media», *SIAM J. Numer. Anal.*, vol 45, n° 5, 2007, p. 2228-2258.
- [DOM 05] DOMELEVO K., OMNES P., «A finite volume method for the Laplace equation on almost arbitrary two-dimensional grids», *M2AN Math. Model. Numer. Anal.*, vol 39, n° 6, 2005, p. 1203–1249.

- [DRO 03] DRONIOU J., «Error estimates for the convergence of a finite volume discretization of convection-diffusion equations», *J. Numer. Math.*, vol 11, n° 1, 2003, p. 1-32.
- [DRO 06-1] DRONIOU J., «Finite volume schemes for fully non-linear elliptic equations in divergence form», *M2AN Math. Model. Numer. Anal.*, vol 40, n° 6, 2006, p. 1069-1100.
- [DRO 06-2] DRONIOU J., EYMARD R., «A mixed finite volume scheme for anisotropic diffusion problems on any grid», *Num. Math.*, vol 105, n° 1, 2006, p. 35-71.
- [DRO 07] DRONIOU J., EYMARD R., «Study of the mixed finite volume method for Stokes and Navier-Stokes equations», to appear in *Numerical Methods for Partial Differential Equations*.
- [EYM 00] EYMARD R., GALLOUËT T., HERBIN R., *Finite Volume Methods*, Handbook of Numerical Analysis, Edited by P.G. Ciarlet and J.L. Lions, North Holland 7, 2000, p. 713–1020.
- [LEP 05] LE POTIER C., «Schéma volumes finis pour des opérateurs de diffusion fortement anisotropes sur des maillages non structurés», *C. R. Math. Acad. Sci. Paris*, vol 340, n° 12, 2005, p. 921–926.
- [QUA 99] QUARTERONI A. AND VALLI A., *Domain Decomposition Methods for Partial Differential Equations*, Oxford Science Publications, 1999.